NDT/NDE by means of a probabilistic differential compressive sensing method

Journal of Physics: Conference Series **1476** (2020) 012006 doi:10.1088/1742-6596/1476/1/012006

NDT/NDE by means of a probabilistic differential compressive sensing method

Giorgio Gottardi, Mohammad Abdul Hannan, and Alessandro Polo

ELEDIA Research Center (ELEDIA@UniTN - University of Trento), Via Sommarive 9, I-38123 Trento, Italy

E-mail: giorgio.gottardi@unitn.it

Abstract. A novel microwave imaging (*MI*) method is proposed to deal with the non-destructive testing and evaluation (*NDT/NDE*) of dielectric structures. The proposed technique exploits a *probabilistic differential* contrast source inversion (*D-CSI*) formulation of the inverse scattering (*IS*) problem, which is then effectively solved by means of a customized multi-task Bayesian compressive sensing (*MT-BCS*) solver. Numerical results are shown to assess the effectiveness and robustness of the proposed *NDT/NDE* method, as well as to compare it with a single-task (*ST-BCS*) implementation within the same framework.

1. Introduction

Microwave imaging (*MI*) is nowadays considered a promising alternative to established technologies such as eddy current testing (*ECT*) [1] and ultrasound testing (*UT*) [2] for *NDT/NDE* purposes [3][4]. However, the structural evaluation of low-permittivity/low-loss media (e.g., glass fiber reinforced polymers, foam, and honeycombs) requires to carefully address challenging issues of the arising inverse scattering (*IS*) problem such as *non-linearity* and *ill-posedness* [5][6].

Linear approximations (e.g., Born or Rytov [7][8]) have been often exploited to restore linearity. However, they can be applied only when weak scatterers have to be imaged, being otherwise suitable to provide only *qualitative* guesses, without *quantitative* material characterization. Alternatively, multi-resolution approaches have been successfully integrated with both deterministic [9] and stochastic solvers to mitigate the occurrence of local minima/false solutions by reducing the ratio between problem unknowns and non-redundant/informative data. On the other hand, proper regularization strategies must be studied to deal with the *ill-posedness* of the *IS* problem [5]. In this context, *a-priori* information on the inspected structure and on the class of imaged targets is an effective recipe to yield stable solutions. When dealing with *NDT/NDE*, generally-available *a-priori* information about the unperturbed structure can be profitably taken into account to re-formulate the *IS* problem in a *differential* framework in order to retrieve only differences with respect to a known scenario [10]. Moreover, knowing the type/shape of scatterers (e.g., cracks) can significantly shrink the solution space, allowing to retrieve specific descriptors (e.g., location and dimensions), as done in recent works on learning-by-examples (*LBE*) parametric inversion methods [11]-[13].

Besides all mentioned approaches, compressive sensing (*CS*)-based methods can yield regularized and computationally-efficient solutions of the *IS* problem when the sought unknowns are *sparse*

(i.e., represented by few non-null coefficients) with respect to a suitable expansion basis [14]-[18]. Accordingly, this work presents a novel *MI* technique for *NDT/NDE* based on a multi-task Bayesian *CS* (*MT-BCS*) solution method [19] exploiting a *probabilistic differential* contrast source inversion (*D-CSI*) formulation of the *IS* problem.

2. *D-CSI* Probabilistic Formulation of the *IS* Problem and *BCS* Solution Method

Let us consider a two-dimensional (*2D*) *NDT/NDE* scenario in which an investigation domain $\mathcal{D}_{inv}$ is probed by V plane waves with known incident electric field distribution $\xi_i^v(x, y)$, $v = 1, ..., V$[1]. The known background medium occupying $\mathcal{D}_{inv}$ is characterized by relative permittivity and conductivity distributions equal to $\varepsilon_{rB}(x, y)$ and $\sigma_B(x, y)$, respectively. Moreover, the scattered radiation is collected at M sampling locations (x_m, y_m), $m = 1, ..., M$, uniformly distributed over an external circular observation domain $\mathcal{D}_{obs}$ of radius R_{obs}.

Assuming a *D-CSI* formulation of the *MI* problem at hand, it is possible to express the *differential* scattered field

$$\Delta\xi^v(x, y) = \xi^v(x, y) - \xi_B^v(x, y); \quad v = 1, ..., V \tag{1}$$

as the difference between the total field in presence of one or multiple unknown scatterers inside $\mathcal{D}_{inv}$, $\xi^v(x, y)$, and the total field for the unperturbed background, $\xi_B^v(x, y)$ [2]. Accordingly, the v-th differential field in $\mathcal{D}_{obs}$ is expressed through the following integral *data* equation [3]

$$\Delta\xi^v(x, y) = \int_{\mathcal{D}_{inv}} G_B(x, y; x', y')\, \Delta J^v(x', y')\, dx'dy'; \quad (x, y) \in \mathcal{D}_{obs};\ v = 1, ..., V \tag{2}$$

where $G_B(x, y; x', y')$ is the *inhomogeneous* Green's function for the known background medium. In (2) $\Delta J^v(x, y)$ is the v-th *differential contrast source*

$$\Delta J^v(x, y) = \xi^v(x, y)\, \Delta\tau(x, y); \quad v = 1, ..., V \tag{3}$$

where

$$\Delta\tau(x, y) = [\varepsilon_{rB}(x, y) - \varepsilon_r(x, y)] - j\left[\frac{\sigma_B(x, y) - \sigma(x, y)}{\omega\varepsilon_0}\right] \tag{4}$$

is the *differential contrast function* mathematically modeling the presence of unknown targets inside $\mathcal{D}_{inv}$ with relative permittivity and conductivity distributions equal to $\varepsilon_r(x, y)$ and $\sigma(x, y)$, respectively.

To numerically deal with the solution of the differential *IS* problem at hand, D_{inv} is discretized into N square sub-domains by means of N pixel basis functions. Accordingly, it is possible to rewrite (2) in compact matrix notation as follows

$$\underline{\Delta\xi}^v = \underline{\underline{G}}_B \underline{\Delta J}^v; \quad v = 1, ..., V \tag{5}$$

where $\underline{\Delta\xi}^v = \{\Delta\xi^v(x_m, y_m);\ m = 1, ..., M\}$ contains the differential scattered field samples, $\underline{\Delta J}^v = \{\Delta J^v(x_n, y_n);\ n = 1, ..., N\}$ is the unknown v-th differential contrast source in each sub-domain, while $\underline{\underline{G}}_B$ is the $(M \times N)$ inhomogeneous Green's operator.

Under the hypothesis that the problem unknowns are *sparse* (i.e., represented by few non-null coefficients) in the selected pixel basis, it is possible to yield a regularized solution of (5) by re-formulating the *IS* problem in a *probabilistic BCS* framework and looking for the maximum *a-posteriori* estimate

$$\underline{\Delta J}^v = \arg\left(\max_{\underline{\Delta J}^v}\left\{\mathcal{P}\left(\underline{\Delta J}^v \middle| \underline{\Delta\xi}^v\right)\right\}\right); \quad v = 1, ..., V. \tag{6}$$

[1] Subscript i stands for *incident*.
[2] Subscript B stands for *background*.
[3] A time dependency factor $\exp(j\omega t)$ is assumed and omitted for notation simplicity.

As a matter of fact, thanks to the *BCS,* sparseness priors can be imposed without the need for checking the compliance of the restricted isometry property (*RIP*) by the inhomogeneous Green's operator (required by standard *CS* algorithms and often unfeasible from a computational point of view, even for small problems [14]). Owing to the availability, to the authors' best knowledge, of *BCS* solvers able to deal only with real linear problems, the data equation (5) is first rewritten by separating the real/imaginary ($\Re/\Im$) parts as follows

$$\underline{\Delta E}^v = \underline{\underline{\mathcal{G}}}_B \underline{\Delta \mathcal{J}}^v; \quad v = 1, ..., V \tag{7}$$

where $\underline{\Delta E}^v = \left\{\Re\left(\underline{\Delta \xi}^v\right); \Im\left(\underline{\Delta \xi}^v\right)\right\}$, $\underline{\Delta \mathcal{J}}^v = \left\{\Re\left(\underline{\Delta J}^v\right); \Im\left(\underline{\Delta J}^v\right)\right\}$, while $\underline{\underline{\mathcal{G}}}_B$ contains the $\Re/\Im$ parts of $\underline{\underline{G}}_B$. Then, a closed form solution of (7), $\underline{\widehat{\Delta \mathcal{J}}}^v = \left\{\widehat{\Delta \mathcal{J}}_n^v; n = 1, ..., 2N\right\}$, is computed according to the *MT-BCS* theory as [19]

$$\underline{\widehat{\Delta \mathcal{J}}}^v = \left[\mathrm{diag}\left(\underline{\widehat{a}}\right) + \underline{\underline{\mathcal{G}}}_B^T \underline{\underline{\mathcal{G}}}_B\right]^{-1} \underline{\underline{\mathcal{G}}}_B^T \underline{\Delta E}^v; \quad v = 1, ..., V \tag{8}$$

where $\underline{\widehat{a}} = (\widehat{a}_n; n = 1, ..., 2N)$ is the set of *MT-BCS* hyper-parameters, shared among all views ($v = 1, ..., V$) to enforce the existing physical correlation among differential currents under several illuminations, computed through a relevance vector machine (*RVM*) solver as

$$\underline{\widehat{a}} = \arg\left\{\max_{\underline{a}}\left[-\frac{1}{2}\sum_{v=1}^{V} 2\left(M + \beta_1\right)\log\left(\left(\underline{\Delta E}^v\right)^T \underline{\underline{K}}^{-1} \underline{\Delta E}^v + 2\beta_2\right) + \log\left|\underline{\underline{K}}\right|\right]\right\} \tag{9}$$

where β_1 and β_2 are *MT-BCS* control parameters and $\underline{\underline{K}} = \underline{\underline{I}} + \underline{\underline{\mathcal{G}}}_B \left[\mathrm{diag}\left(\underline{a}\right)\right]^{-1} \left(\underline{\underline{\mathcal{G}}}_B\right)^T$, $.^T$ and $|.|$ are the transpose and the determinant, respectively, and $\underline{\underline{I}}$ is the identity matrix. Finally, the differential contrast is retrieved as

$$\widehat{\Delta\tau}\left(x_n, y_n\right) = \frac{1}{V}\sum_{v=1}^{V} \frac{\widehat{\Delta \mathcal{J}}_n^v + j\widehat{\Delta \mathcal{J}}_{n+N}^v}{\widehat{\xi}^v\left(x_n, y_n\right)}; \quad n = 1, ..., N \tag{10}$$

where $\widehat{\xi}^v\left(x_n, y_n\right)$ is the retrieved total field in the n-th cell belonging to $\mathcal{D}_{inv}$.

3. Numerical Assessment

To numerically assess the proposed *MT-BCS* methodology, a square investigation domain of side 2λ probed by $V = 18$ plane waves impinging from angular directions $\phi^v = (v-1)\frac{2\pi}{V}$, $v = 1, ..., V$, has been considered as reference benchmark scenario. The scattered field has been collected over $M = 18$ ideal receivers ($R_{obs} = 2\lambda$), while $N = 400$ pixel basis functions have been considered to solve the inverse problem.

Figure 1 shows the *MT-BCS* reconstruction when dealing with the retrieval of a set of small cracks embedded within a lossless background with relative permittivity $\varepsilon_{rB} = 1.1$ [$\Delta\tau = 0.1$ - Fig. 1(a)] and processing blurred data with a signal-to-noise ratio of $SNR = 20$ dB. As it can be observed, all scatterers have been correctly detected, and a faithful reconstruction of their support and contrast function has been yielded [Fig. 1(b) vs. Fig. 1(a)]. Moreover, there is a clear advantage of the *MT-BCS* over a "simpler" single-task *BCS* (*ST-BCS*) solution approach [14] formulated within the *D-CSI* framework [Fig. 1(b) vs. Fig. 1(c)]. As a matter of fact, although relying on the same probabilistic framework, the *ST-BCS* does not enforce any correlation among several views in solving (6), resulting in a significantly worse guess of the defects inside $\mathcal{D}_{inv}$ [Fig. 1(c)].

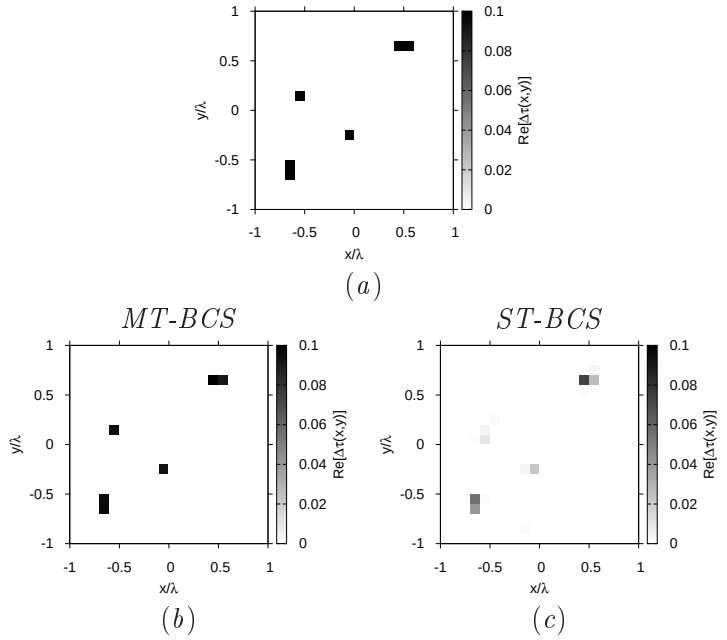

Figure 1. *Numerical Assessment* ("*Random Cracks*", $\Delta\tau = 0.1$, $SNR = 20$ dB) - (a) Actual and retrieved differential contrast by the (b) *MT-BCS* and (c) *ST-BCS* methods.

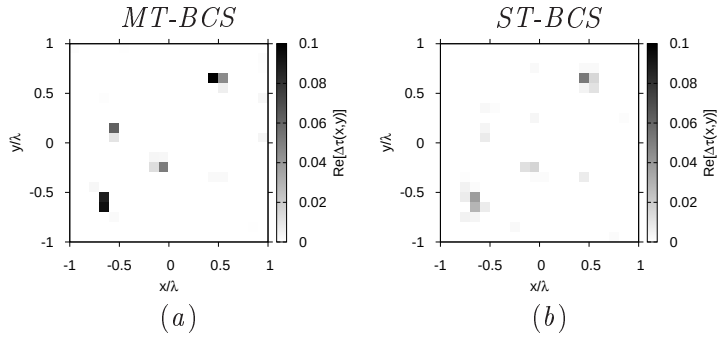

Figure 2. *Numerical Assessment* ("*Random Cracks*", $\Delta\tau = 0.1$, $SNR = 5$ dB) - (a) Actual and retrieved differential contrast by the (b) *MT-BCS* and (c) *ST-BCS* methods.

Such positive outcomes are confirmed when processing highly blurred data, as well. Indeed, the plot of the *MT-BCS* [Fig. 2(a)] and *ST-BCS* [Fig. 2(b)] solutions when $SNR = 5$ dB verify the superior performance of the proposed methodology regardless of the harsh operative conditions. Moreover, it is worth pointing out that the *MT-BCS* solutions come at a higher computational efficiency with respect to the *ST-BCS* ones (i.e., $\Delta t|_{MT-BCS} = 20$ [sec] vs. $\Delta t|_{ST-BCS} = 37$ [sec]). This is in agreement with the reference literature, since the *MT-BCS* processes all multi-view data in a single inversion stage, while multiple inversions are performed by the *ST-BCS* to invert scattered data related to V illuminations [17].

To further investigate the robustness and reliability of the proposed *NDT/NDE* solution approach, let us now consider the retrieval of the vertical crack in Fig. 3(a) [4].

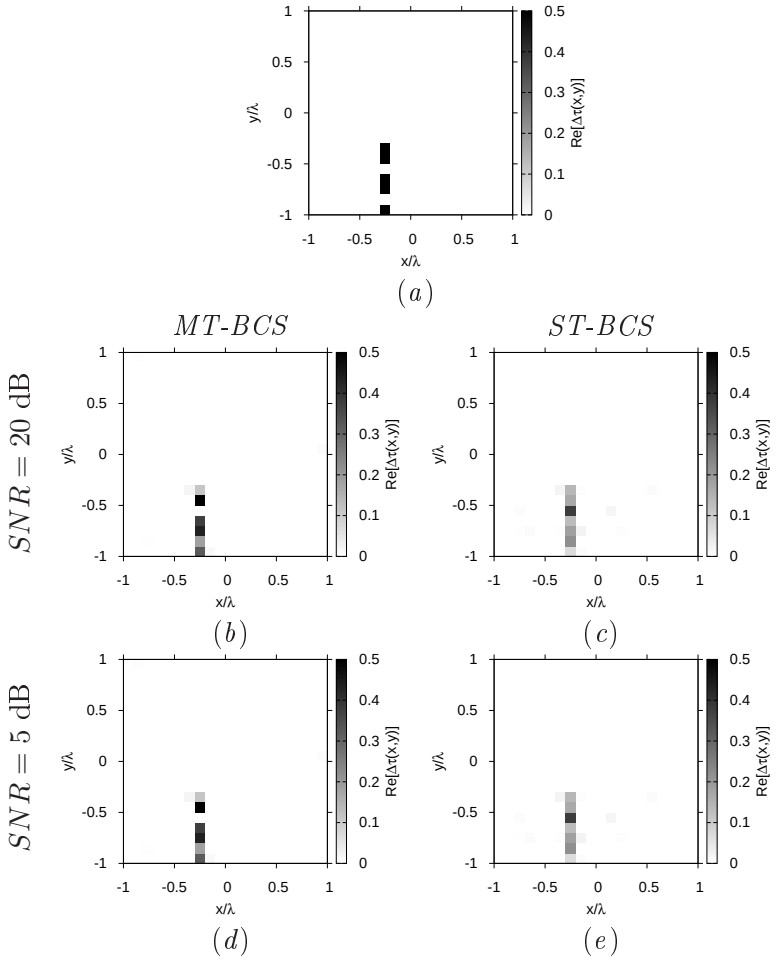

Figure 3. *Numerical Assessment* ("*Vertical Crack*", $\Delta\tau = 0.5$, $SNR \in \{5, 20\}$ dB) - (a) Actual and retrieved differential contrast by the (b)(d) *MT-BCS* and (c)(e) *ST-BCS* methods when processing noisy data at (b)(c) $SNR = 20$ dB and (d)(e) $SNR = 5$ dB.

The background medium has a relative permittivity of $\varepsilon_{rB} = 1.5$, yielding a differential contrast of $\Delta\tau = 0.5$. As it can be observed, the *MT-BCS* overcomes the *ST-BCS* whatever the level of noise on scattered data. As a matter of fact, the *ST-BCS* under-estimates the contrast and provides less accurate reconstructions of the target support, with a larger amount of artifacts in the background [e.g., Fig. 3(e) vs. Fig. 3(d) - $SNR = 5$ dB].
To conclude, the plot of the total reconstruction error

$$\gamma_{tot} = \frac{1}{Area\left(\mathcal{D}_{inv}\right)} \int_{\mathcal{D}_{inv}} \frac{\left|\Delta\tau\left(x,\, y\right) - \widehat{\Delta\tau}\left(x,\, y\right)\right|}{\left|\Delta\tau\left(x,\, y\right) + 1\right|} dxdy \tag{11}$$

[4] It is worth pointing out that the selected test case is aimed at assessing the effectiveness of the proposed method also when the unknown defect is not a collection of disconnected pixels randomly distributed within the imaged domain as in the previous example.

has been reported in Fig. 4 as a function of the background relative permittivity. As expected, there is a progressive degradation of the "quality" of both ST/MT solutions as ε_{rB} increases, given the higher value of the differential contrast. However, the reported results confirm that the MT-BCS always yields significant improvements of the retrieved images with respect to its ST counterpart.

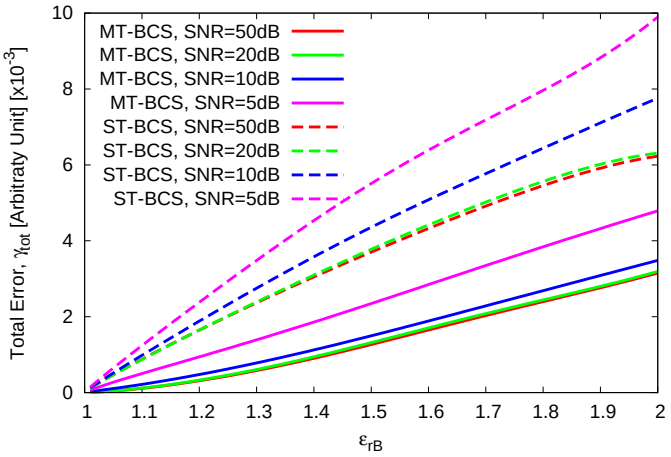

Figure 4. *Numerical Assessment* ("*Vertical Crack*", $SNR \in [5, 50]$ dB) - Behavior of total reconstruction error as a function of the background relative permittivity for the MT-BCS and ST-BCS methods.

4. Conclusions

An innovative sparseness promoting approach to deal with the NDT/NDE of dielectric structures has been presented. The proposed MT-BCS approach is based on a probabilistic D-CSI formulation of the IS problem allowing to effectively exploit (a) generally-available *a-priori* information of the unperturbed/healthy scenario, (b) sparseness priors on the class of imaged targets, as well as (c) the existing correlation between differential contrast sources under several illuminations. It is worth remarking that the underlying hypothesis of the sparseness of the unknowns with respect to the pixel basis may not be appropriate to model large defects such as delaminations. However, the approach is general and could be in principle applied exploiting alternative (i.e., more suitable) expansion bases (e.g., wavelets [18]). The reported results have shown that the MT-BCS provides faithful reconstructions under several operative conditions, overcoming a ST implementation based on the same formulation. Future works will be aimed at further assessing the suitability of the proposed methodology also for the NDT/NDE of specimens with higher permittivity values with respect to those considered in this paper, which are representative of low-permittivity materials such as foams, honeycombs, and glass fiber reinforced polymers [20]. Moreover, the retrieval of non-crack defects (e.g., with losses as well as characterized by inhomogeneous permittivity distributions) will be carefully investigated.

Acknowledgments

This work benefited from the networking activities carried out within the SNATCH Project (2017-2019) funded by the Italian Ministry of Foreign Affairs and International Cooperation, Directorate General for Cultural and Economic Promotion and Innovation, the Project "CYBER-PHYSICAL ELECTROMAGNETIC VISION: Context-Aware Electromagnetic Sensing and Smart Reaction (EMvisioning)" funded by the Italian Ministry of Education, University, and

Research within the PRIN2017 Program, and the Project "WATERTECH - Smart Community per lo Sviluppo e l'Applicazione di Tecnologie di Monitoraggio Innovative per le Reti di Distribuzione Idrica negli usi idropotabili ed agricoli" (Grant no. SCN_00489) funded by the Italian Ministry of Education, University, and Research within the Program "Smart cities and communities and Social Innovation" (CUP: E44G14000060008).

References

[1] Miorelli R, Reboud C, Lesselier D Theodoulidis T 2012 Eddy current modeling of narrow cracks in planar-layered metal structures *IEEE Trans. Magn.* **48** 2551-2559
[2] Dobie G, Summan R, Pierce S G, Galbraith W and Hayward G 2011 A noncontact ultrasonic platform for structural inspection *IEEE Sensors J.* **11** 2458-2468
[3] Kharkovsky S and Zoughi R 2007 Microwave and millimeter wave nondestructive testing and evaluation - Overview and recent advances *IEEE Instrum. Meas. Mag.* **10** 26-38
[4] Mudanyali O, Yildiz S, Semerci O, Yapar A and Akduman I 2008 A microwave tomographic approach for nondestructive testing of dielectric coated metallic surfaces *IEEE Geosci. Remote Sens. Lett.* **5** 180-184
[5] Chen X 2018 *Computational Methods for Electromagnetic Inverse Scattering* (Singapore: Wiley-IEEE)
[6] Zhong Y, Lambert M, Lesselier D and Chen X 2016 A new integral equation method to solve highly nonlinear inverse scattering problems *IEEE Trans. Antennas Propag.* **64** 1788-1799
[7] Slaney M, Kak AC and Larsen LE 1984 Limitations of imaging with first-order diffraction tomography *IEEE Trans. Microw. Theory Techn.* **32** 860-874
[8] Shumakov D and Nikolova N 2018 Fast quantitative microwave imaging with scattered-power maps *IEEE Trans. Microw. Theory Techn.* **66** 439-449
[9] Salucci M, Poli L and Massa A 2017 Advanced multi-frequency GPR data processing for non-linear deterministic imaging *Signal Proc.* **132** 306-318
[10] Xu K, Zhong Y, Chen X and Lesselier D 2018 A fast integral equation-based method for solving electromagnetic inverse scattering problems with inhomogeneous background *IEEE Trans. Antennas Propag.* **66** 4228-4239
[11] Salucci M, Anselmi N, Oliveri G, Calmon P, Miorelli R, Reboud C and Massa A 2016 Real-time NDT-NDE through an innovative adaptive partial least squares SVR inversion approach *IEEE Trans. Geosci. Remote Sensing* **54** 6818-6832
[12] Salucci M, Anselmi N, Oliveri G, Rocca P, Ahmed S, Calmon P, Miorelli R, Reboud C and Massa A 2019 A nonlinear kernel-based adaptive learning-by-examples method for robust NDE-NDT of conductive tubes *J. Electromagn. Waves Appl.* (in press, DOI: 10.1080/09205071.2019.1572546)
[13] Massa A, Oliveri G, Salucci M, Anselmi N and Rocca P 2018 Learning-by-examples techniques as applied to electromagnetics *J. Electromagn. Waves Appl.* **32** 516-541
[14] Oliveri G, Salucci M, Anselmi N and Massa A 2017 Compressive sensing as applied to inverse problems for imaging: theory, applications, current trends, and open challenges *IEEE Antennas Propag. Mag.* **59** 34-46
[15] Helander J, Ericsson A, Gustafsson M, Martin T, Sjoberg D and Larsson C 2017 Compressive sensing techniques for mm-wave nondestructive testing of composite panels *IEEE Trans. Antennas Propag.* **65** 5523-5531
[16] Anselmi N, Oliveri G, Hannan M A, Salucci M and Massa A 2017 Color compressive sensing imaging of arbitrary-shaped scatterers *IEEE Trans. Microwave Theory Techn.* **65** 1986-1999
[17] Salucci M, Gelmini A, Poli L, Oliveri G and Massa A 2018 Progressive compressive sensing for exploiting frequency-diversity in *GPR* imaging *J. Electromagn. Waves Appl.* **32** 1164-1193
[18] Anselmi N, Oliveri G, Salucci M and Massa A 2015 Wavelet-based compressive imaging of sparse targets *IEEE Trans. Antennas Propag.* **63** 4889-4900
[19] Ji S, Dunson D and Carin L 2009 Multitask compressive sensing *IEEE Trans. Signal Process.* **57** 92-106
[20] Viegas C et *al* 2017 Active millimeter-wave radiometry for nondestructive testing/evaluation of composites-glass fiber reinforced polymer *IEEE Trans. Microw. Theory Techn.* **65** 641-650